

See discussions, stats, and author profiles for this publication at: <https://www.researchgate.net/publication/263959060>

# A New Microcrystalline Phytosterol Polymorph Generated Using CO<sub>2</sub>-Expanded Solvents

ARTICLE *in* CRYSTAL GROWTH & DESIGN · NOVEMBER 2013

Impact Factor: 4.89 · DOI: 10.1021/cg401068n

---

CITATIONS

4

---

READS

62

## 6 AUTHORS, INCLUDING:



Evelyn Moreno-Calvo  
Spanish National Research Council  
31 PUBLICATIONS 239 CITATIONS

[SEE PROFILE](#)



Norberto Masciocchi  
Università degli Studi dell'Insubria  
264 PUBLICATIONS 5,557 CITATIONS

[SEE PROFILE](#)



Jaume Veciana  
Spanish National Research Council  
983 PUBLICATIONS 12,414 CITATIONS

[SEE PROFILE](#)



Nora Ventosa  
Materials Science Institute of Barcelona  
106 PUBLICATIONS 1,242 CITATIONS

[SEE PROFILE](#)

# A New Microcrystalline Phytosterol Polymorph Generated Using CO<sub>2</sub>-Expanded Solvents

Evelyn Moreno-Calvo,<sup>†,§</sup> Feral Temelli,<sup>\*,†,‡</sup> Alba Cordoba,<sup>§,†</sup> Norberto Masciocchi,<sup>||</sup> Jaume Veciana,<sup>†,§</sup> and Nora Ventosa<sup>\*,†,§</sup>

<sup>†</sup>Department of Molecular Nanoscience and Organic Materials, Institut de Ciència de Materials de Barcelona (ICMAB- CSIC), Campus de la Universitat Autònoma de Barcelona (UAB), 08193 Bellaterra, Spain

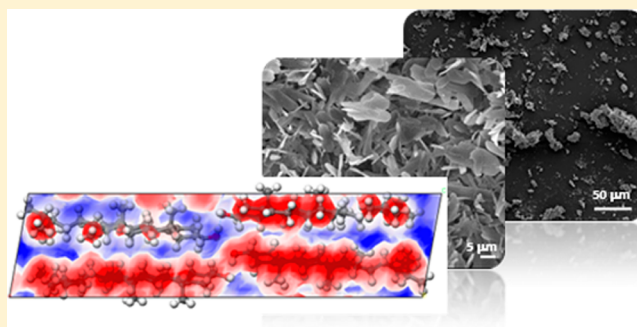
<sup>‡</sup>Department of Agricultural, Food and Nutritional Science, University of Alberta, Edmonton, Alberta, Canada T6G 2PS

<sup>§</sup>CIBER de Bioingeniería, Biomateriales y Nanomedicina (CIBER-BBN)

<sup>||</sup>CIBER de Bioingeniería, via Valleggio 11, 22100 Como, Italy

## Supporting Information

**ABSTRACT:** Phytosterols have been receiving increasing attention due to their demonstrated health benefits. Micronization of phytosterol particles is desirable to enhance their physiological efficacy. Utilization of the environmentally friendly compressed fluid-based technology, called Depressurization of an Expanded Liquid Organic Solution (DELOS) was investigated to micronize a phytosterol mixture. A new polymorph of  $\beta$ -sitosterol, which was more crystalline than the native form, was obtained from the DELOS process regardless of the process conditions. In addition, particle size was reduced by an order of magnitude. The crystal structure of the new polymorph was determined from X-ray powder diffraction data. The proposed crystal structure for  $\beta$ -sitosterol, which contains a number of nearly isosteric vicariant molecules of lower molecular weight (mostly campesterol and campestanol, accounting in a crystalline solid-solution for nearly 10% of the molecular mixture) allows the presence of small cavities, in which some residual solvent molecules are temporarily trapped. Further structural analysis of the new and native polymorphs were performed by laser diffractometry, scanning electron microscopy, differential scanning calorimetry, thermogravimetric analysis, and X-ray powder diffraction. Findings of the study provide a route to obtain nutraceutical products that might show enhanced functional properties.



## 1. INTRODUCTION

Dietary treatment of hypercholesterolemia has been receiving increasing attention, which has led to the rapid growth of functional food and nutraceutical products, incorporating ingredients targeting cholesterol reduction. One type of such ingredient is phytosterols. Their structures are similar to that of cholesterol but each phytosterol has an additional side chain (Figure 1). Examples of some common phytosterols are  $\beta$ -sitosterol (cholesterol with the inclusion of an extra ethyl group at the C-24 position), campesterol (cholesterol with the inclusion of an extra methyl group at the C-24 position), and stigmasterol (cholesterol with the inclusion of an additional ethyl group at the C-24 position and double bond at the C-22 position). Phytosterols are divided into two main subgroups, namely "phytosterols" and "phytstanols", the latter formed by reduction of the double bond in the sterol ring structure at the C-5 position.

A meta-analysis of 41 clinical trials have demonstrated the effectiveness of phytosterols and phytstanols in decreasing low-density lipoprotein (LDL) cholesterol by about 10% at an intake level of 2 g/day.<sup>1</sup> This evidence has led to the approval

of a health claim by the U.S. Food and Drug Administration (FDA), indicating that foods containing at least 0.65 g per serving of plant sterol esters, (or 1.7 g of stanol esters) eaten twice a day, as part of a diet low in saturated fat and cholesterol, may reduce the risk of heart disease.<sup>2,3</sup> Indeed, a recent study by G. Jahreis, et al.<sup>4</sup> has demonstrated the reduction of cholesterol levels in Dunkin Hartley guinea pigs fed with a sitosterol supplement. Compared to a high-cholesterol diet, all diets supplemented with sitosterol formulations decreased liver cholesterol concentrations.

Phytosterols are absorbed to a much smaller extent in the body compared to cholesterol and they interfere with the intestinal absorption of cholesterol.<sup>1</sup> As part of the digestion process, cholesterol is first incorporated into dietary mixed micelles for absorption in the intestine. Phytosterols, which are relatively more hydrophobic than cholesterol, are in a dynamic competition with cholesterol for incorporation into dietary

**Received:** July 15, 2013

**Revised:** October 2, 2013

**Published:** October 16, 2013



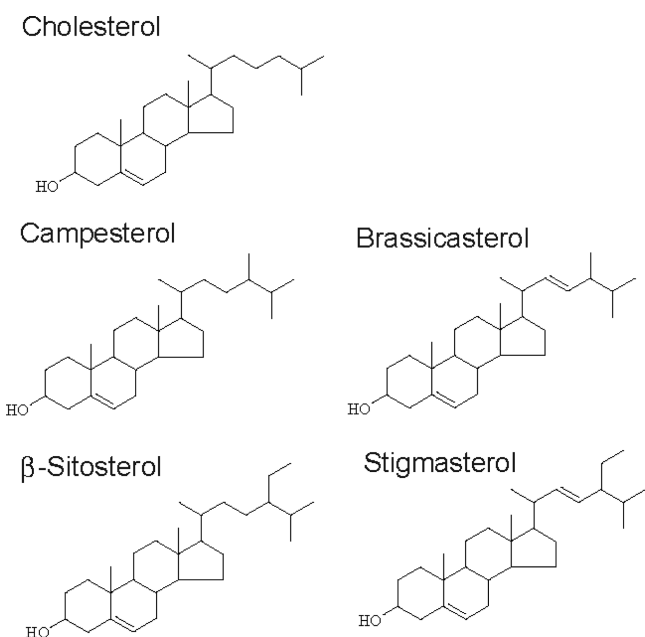


**Figure 1.** Chemical structures of cholesterol and the main components of the phytosterol mixture. Stanols are saturated sterols, having no double bonds in the sterol ring structure.

mixed micelles, displacing cholesterol and leading to its enhanced excretion.<sup>5,6</sup> Nonetheless, as discussed by Rozner and Garti,<sup>7</sup> work continues on understanding the mechanism by which phytosterols lower serum cholesterol levels so that those same reductions may be achieved using smaller phytosterol doses.

Phytosterols are not synthesized by the human body and have to be consumed as part of the diet.<sup>8</sup> In the human diet, vegetable oils, cereal grains, and nuts are the richest sources of phytosterols.<sup>9</sup> With the growing market demands, phytosterols are isolated commercially from vegetable oil deodorizer distillates or tall oil in the form of a mixture of sterol components, the separation of which presents a major challenge.

With such complexity of the phytosterol mixtures and small differences in their physicochemical properties, the efficacy of various phytosterol preparations has been variable. Efficacy was found to be similar for phytosterols and phytostanols.<sup>1</sup> However, poorly soluble, crystalline forms used in the earlier studies have not been very effective in reducing cholesterol due to the limitations of their inclusion into the micellar phase, requiring much larger doses.<sup>9</sup> It was stated that the free/unesterified form could be just as effective as the esterified form; however, the delivery form and the food matrix were very important.<sup>1</sup> Small crystals with increased surface area would facilitate saturation of the intestinal lumen and thus be more effective in the replacement of cholesterol in dietary mixed micelles, interfering with cholesterol absorption.<sup>10,11</sup>

Incorporation of phytosterols into food product formulations has been very challenging because phytosterols/stanols are high-melting crystalline powders that are not soluble in water and hardly soluble in fats and oils (2–3% solubility in oil at 298 K<sup>12</sup>). Crystallization of sterols in the oil phase would lead to gritty texture, compromising sensory quality and consumer acceptability as well as efficacy. Therefore, sterol/stanol esters have been used to a greater extent successfully since they are in liquid or semiliquid form that can be incorporated easily into

high-fat products, like margarines and spreads. However, enrichment of low-fat products is still a challenge since the taste of the product can be affected negatively if the sterol esters are distributed only in the small amount of fat in the product.<sup>12</sup>

On the basis of the above, it is desirable to have small crystals of unbound sterols, in order to decrease the required daily dose. It is also desirable for these formulations to be easily dispersible in water to allow their incorporation into a wider range of food products, including low-fat formulations.<sup>13</sup> Different approaches investigated to develop effective delivery forms for phytosterols include micronization of crystals and formation of emulsions and liposomes. Decreasing the particle size by micronization increases the surface-to-volume ratio, leading to increased solubilization and thus increased bioavailability. Christiansen et al.<sup>10</sup> prepared a microcrystalline  $\beta$ -sitosterol suspension in oil and water, whereas Rossi et al.<sup>11</sup> used water as an antisolvent to form colloidal phytosterol particles from an ethanol solution in the presence of a nonionic surfactant, Tween 80. Both of these approaches require vigorous mixing to control the growth rate of particles, which is a challenge for large-scale operations. Incorporation of phytosterols into microemulsions through various emulsification approaches made it possible to incorporate phytosterols into water-based food product formulations.<sup>14–16</sup> Such forms have been shown to be more effective for cholesterol reduction than sterol esters.<sup>17,18</sup>

Supercritical carbon dioxide (SC-CO<sub>2</sub>) technology, where CO<sub>2</sub> is used as a solvent at temperature and pressure conditions above its critical point (304.1 K and 7.4 MPa) has been employed for the recovery of phytosterols from different sources, especially by fractionation of deodorizer distillates from sunflower<sup>19</sup> and soy<sup>20</sup> after enzymatic modification to form esters, as well as canola deodorizer distillate<sup>21</sup> and rice bran oil<sup>22</sup> with the use of a supercritical fractionation column. However, the use of supercritical fluid technologies for phytosterol particle engineering has been scarce.<sup>23</sup> A modified form of the rapid expansion of the supercritical solutions (RESS) technique was used by Turk et al.<sup>24</sup> to form composite L-poly(lactic acid)-phytosterol particles, where both phytosterols and the polymer were first dissolved in SC-CO<sub>2</sub> followed by coprecipitation. Turk and Leitzow<sup>25</sup> described the RESSAS (rapid expansion of supercritical solution to aqueous solution) process, where the supercritical solution of CO<sub>2</sub> + phytosterols was expanded into an aqueous solution containing a surfactant. Even though these processes may produce particles of very small size (aggregates of 50 nm particles), the main limitation for scale up would be the very low solubility of phytosterols in SC-CO<sub>2</sub>.

Another promising approach taking advantage of the tunable properties of compressed fluids and gas-expanded liquids is the DELOS (depressurization of an expanded liquid organic solution) process, where CO<sub>2</sub> acts as a cosolvent under high pressure.<sup>26</sup> The solute is first dissolved in a conventional organic solvent, and CO<sub>2</sub> is added to volumetrically expand the liquid solution at high pressure. Rapid reduction of pressure to the atmospheric level produces a large, fast, and homogeneous temperature drop, resulting in the formation of micrometer- and submicrometer-sized particles with a narrow particle size distribution.<sup>26</sup> The DELOS process has been used previously to obtain different molecular actives in the form of micropowders, such as 1,4-bis-(*n*-butylamino)-9,10-anthraquinone<sup>26</sup> and stearic acid,<sup>27</sup> as well as various active pharmaceutical compounds like acetylsalicylic acid, acetaminophen, ibuprofen, and

naproxen,<sup>28,29</sup> but not for phytosterols. Our previous work focused on the phase behavior of phytosterol–ethanol–CO<sub>2</sub> mixtures and demonstrated the cosolvent behavior of CO<sub>2</sub> over a wide concentration range of up to around 0.8 mol fraction at 10 MPa and temperatures of 298 and 308 K.<sup>30</sup> Therefore, the DELOS methodology has the potential to process phytosterols into micrometer/submicrometer particles, which was not possible with conventional technologies. The objective of this study was to utilize the DELOS methodology for micronization of phytosterols and to characterize the polymorphism of the particles obtained, including their crystal structures. The feasibility to obtain the same polymorph under different processing conditions of initial solution concentration and CO<sub>2</sub> level was also explored. These preparation processes have been performed by the Biomaterial processing and Nanostructuring Unit (<http://icmab.es/preparation-characterization-of-soft-materials>) of the Institute of Materials Science of Barcelona (ICMAB-CSIC) and the Biomedical Networking Center (CIBER-BBN).

## 2. MATERIALS AND METHODS

**2.1. Materials.** The phytosterol mixture (Arboris Sterols AS-2) was kindly provided by Arboris Pine Tree Extracts (Savannah, GA). The composition of the native phytosterol mixture is provided in Table 1 as

**Table 1. Composition of Phytosterol Mixture As Provided by the Supplier**

	wt %	MW	mp <sup>a</sup>
cholesterol	<0.25%	385.65	149
brassicasterol	<0.5%	398.66	148
campesterol	7.5	400.63	158
campestanol	1.3	402.65	
stigmastanol	0.7	412.69	170
β-sitosterol	76.5	414.71	140
β-sitostanol	11.3	416.73	
other sterols	2.9		

<sup>a</sup>Melting point of phytosterols as reported by Armstrong and Carey<sup>45</sup>

specified by the supplier (see Figure 1 for chemical structures). The average molecular weight of 413.68 g/mol was calculated for the five major components present and then the total was normalized for 100%. This average molecular weight value was used in all the calculations throughout this study. CO<sub>2</sub> (purity 99.995%) was supplied by Carburos Metálicos S.A.–Air Products (Barcelona, Spain). High-performance liquid chromatography (HPLC)-grade ethanol (Ethanol absolute, 99.8%, water <0.1%, residue <0.0001%) was purchased from Teknokroma S. Coop Ltd., Barcelona, Spain, and β-sitosterol (97% purity) was from Sigma-Aldrich (Madrid, Spain).

**2.2. DELOS System and Experimental Design.** The system used for carrying out the DELOS experiments is equipped with a 100 mL vessel (Autoclave Engineers, Wexford, Ireland), a magnedrive stirrer (Autoclave Engineers, Wexford, Ireland) and a syringe pump for the delivery of CO<sub>2</sub> (model 260D, Teledyne Isco Inc., Lincoln, NE). Details of similar systems have been described previously.<sup>26,31</sup> DELOS crystallization experiments of phytosterol mixture, schematically represented in Figure 2, were carried out as follows: A solution of phytosterol in ethanol was prepared at a given initial concentration (C<sub>I</sub>). An appropriate amount of this solution was placed in the high-pressure vessel to give the targeted phytosterol–ethanol–CO<sub>2</sub> mixture composition. Additional known quantity of solid phytosterols was added into the vessel to achieve oversaturated solutions with C<sub>I</sub> values greater than or equal to the saturation concentration (C<sup>S</sup>) at the working temperature. The stirrer was turned on at a rate of 400 rpm. Working temperature (T<sub>w</sub>) was allowed to equilibrate at the desired level (298 or 308 K) with the use of the heater around the vessel and

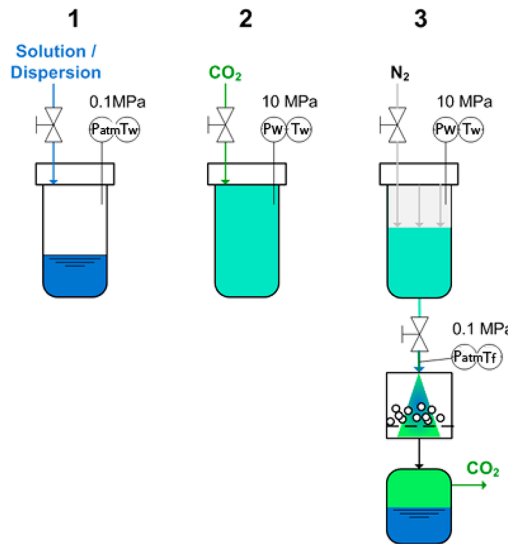


**Figure 2.** Different steps of a DELOS process: (1) Solution of the phytosterol mixture in ethanol is added to the autoclave. (2) Addition of CO<sub>2</sub> produces a new expanded liquid solution which fills all the autoclave volume at a given pressure, P<sub>w</sub>, and temperature, T<sub>w</sub>, giving rise to a solution with a molar fraction of CO<sub>2</sub> given by X<sub>CO<sub>2</sub></sub>. (3) Depressurization of the expanded liquid solution through a nonreturn simple valve, leading to a large, fast, and homogeneous temperature decrease from the working temperature (T<sub>w</sub>) to a final temperature (T<sub>f</sub>), causing precipitation of micrometer-sized particles of phytosterol.

the controller it is attached to. CO<sub>2</sub> was then pumped into the cell until the working pressure (P<sub>w</sub>) of 10 MPa was reached and stabilized, at which time the inlet valve was closed. To calculate the mole fraction of CO<sub>2</sub> (X<sub>CO<sub>2</sub></sub>, solute-free basis), the actual amount of CO<sub>2</sub> introduced to the system was determined by recording the initial and final volumes of the syringe displayed on the pump controller and multiplying by the CO<sub>2</sub> density at the corresponding temperature and pressure of the pump syringe. CO<sub>2</sub> density values were obtained from the NIST Chemistry WebBook.<sup>32</sup> The mixture was stirred and allowed to equilibrate for 1 h. Then, the stirrer was stopped and the inlet valve for nitrogen was opened to allow nitrogen at 10 MPa to push the solution out and to keep the pressure constant, avoiding precipitation in the vessel during the depressurization step. To capture any potentially precipitated material due to the antisolvent effect of CO<sub>2</sub>, especially during those runs performed at conditions close to the phase boundary, a filter (0.2 μm, PTFE filter, Teknokroma, Barcelona, Spain) was placed after the exit valve of the vessel. The solution was then depressurized from P<sub>w</sub> to atmospheric pressure through a nonreturn valve. Upon depressurization, there is a substantial drop in temperature, reaching a final value (T<sub>f</sub>), which was recorded with a thermocouple for the calculation of ΔT = T<sub>f</sub> – T<sub>w</sub>. Upon depressurization, the mother liquor containing the precipitated particles was collected in a container, which was immediately filtered using an offline vacuum filtration set up with 0.2 μm PTFE filter (Teknokroma, Barcelona, Spain). This protocol was adopted based on initial trial runs, which showed that only a small portion of the particles were collected when online filtration set up was used. The collected particles were air-dried followed by leaving them for 4 days in a vacuum chamber at ambient temperature (296 K) before gravimetric determination of their weight and ensuring that constant weight was reached.

On the basis of the phytosterol solubility curve in ethanol–CO<sub>2</sub> mixtures at 10 MPa and 298 K (continuous line in Figure 3) obtained in a previous study,<sup>30</sup> three sets of experiments were performed, as follows: (a) keeping initial concentration (C<sub>I</sub>) constant at 1.7 × 10<sup>-3</sup>, below saturation limit of phytosterol mixture in ethanol and varying X<sub>CO<sub>2</sub></sub> over the range of 0.35–0.80 (experiments DELOS1 to DELOSS, dashed-point line in Figure 3), (b) keeping initial concentration (C<sub>I</sub>)

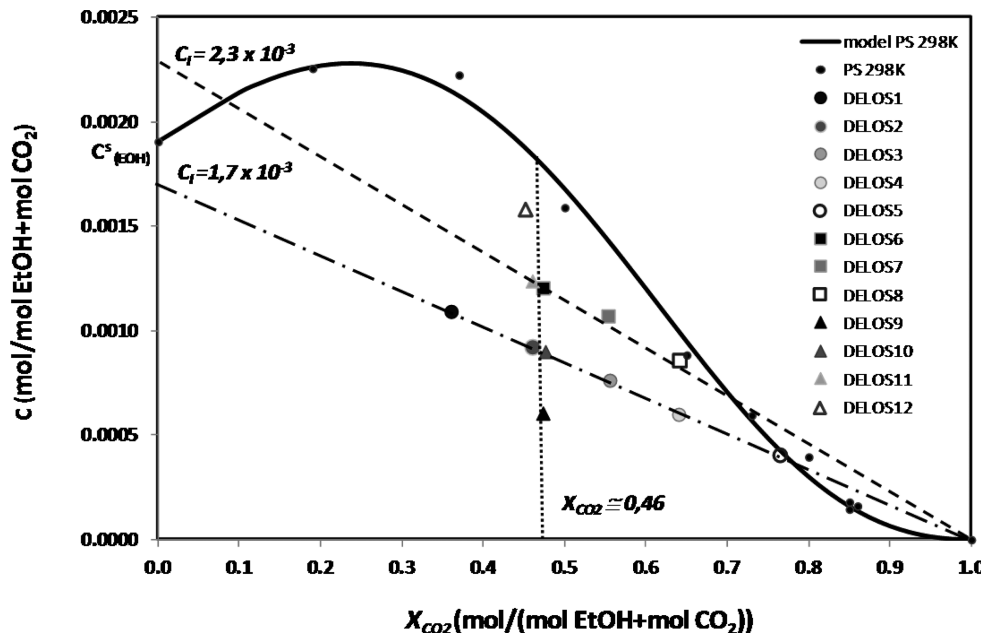


**Figure 3.** Phytosterol solubility curve (continuous line) fitted through experimental solubility data (·) of the phytosterol mixture in  $\text{CO}_2$ -expanded ethanol at 298 K and 10 MPa upon  $X_{\text{CO}_2}$  variation (found in ref 30). Dashed and dashed-point lines connect experiments performed at  $C_1$  of  $2.3 \times 10^{-3}$  and  $1.7 \times 10^{-3}$ , respectively. Dotted line connect experiments performed at the same  $X_{\text{CO}_2}$  of 0.46. For each experiment listed in Table 2, the values of  $C_1$  and  $X_{\text{CO}_2}$  in the  $\text{CO}_2$ -expanded solution are depicted as points in the graph.

constant at  $2.3 \times 10^{-3}$ , above the saturation limit of phytosterol mixture in ethanol and varying  $X_{\text{CO}_2}$  from 0.46 to 0.65 (experiments DELOS6 to DELOS8, dashed line in Figure 3), and (c) keeping  $X_{\text{CO}_2}$  constant at 0.46 and varying  $C_1$  over the range of  $1.1 \times 10^{-3}$  to  $2.3 \times 10^{-3}$  (experiments DELOS9 to DELOS12, dotted line in Figure 3). Two additional experiments were performed at 308 K at  $C_1 = 2.3 \times 10^{-3}$  (DELOS13) and  $3.8 \times 10^{-3}$  (DELOS14) mol phytosterol/mol ethanol.

**2.3. Characterization of Particles.** **2.3.1. Particle Size Analysis.** Particle size distribution of the phytosterol particles was measured with a laser diffraction particle size analyzer (Mastersizer 2000, Malvern Instruments, Worcestershire, U.K.). Samples (20 mg) were dispersed in 20 mL of water, containing 0.05% (w/w) of polyoxyethylene sorbitan monooleate (Tween 80) as a dispersing medium. The suspension was sonicated for 30 min before each measurement.

**2.3.2. Scanning Electron Microscopy (SEM).** The morphology of DELOS-processed phytosterols was studied using a field emission scanning electron microscope (Quanta 200 FEG-SEM, FEI, Eindhoven, The Netherlands). The samples were directly mounted on a biadhesive carbon sheet and coated with gold for 4 min using a sputter coater (K550x, Emitech, Ashford, U.K.) prior to analysis.

**2.3.3. Thermal Analysis.** Differential scanning calorimetry (DSC) measurements were performed with a DSC 8500 (Perkin-Elmer, Madrid, Spain) calorimeter. Samples (4.7–5.0 mg) loaded into 30  $\mu\text{L}$  aluminum pans with a pinhole were heated, cooled, and heated again from 298 to 433 K at a constant rate of 5 K/min. The systematic uncertainties of temperature and heat flow calibration coefficients for the DSC were evaluated as  $\pm 0.2$  K and 2%, respectively. The random part of the uncertainties associated with each measurement was calculated according to the Student's *t* test with a threshold of 95% reliability. The instrument was calibrated using indium and zinc as external standards.

Thermogravimetric analyses (TGA) were performed with a STA 449-F1 Jupiter system (NETZSCH, Selb, Germany), using the NETZSCH Proteus software. Samples of approximately 10 mg were weighed into 100  $\mu\text{L}$  aluminum pans and heated at 5 K/min from 298 to 473 K, under nitrogen (60 mL/min).

**2.3.4. X-ray Powder Diffraction (XRPD) Analysis.** Diffraction patterns were recorded on a Siemens D5000 powder diffractometer (Bragg–Brentano geometry, Munich, Germany), using  $\text{Cu K}\alpha$

radiation ( $\lambda = 1.5406 \text{ \AA}$ ) at a voltage of 40 kV and an intensity of 35 mA. Samples were mounted on a flat glass sample holder and were scanned in the reflection mode from  $2^\circ$  to  $60^\circ$  of  $2\theta$  at a scan rate of  $0.02^\circ$   $2\theta/\text{s}$ .

**2.3.5. Structure Determination from X-ray Powder Diffraction Analysis.** A sample of phytosterols crystallized using the DELOS process was gently ground in an agate mortar and then deposited in the hollow of a 0.2 mm deep aluminum sample holder, equipped with a quartz monocrystal zero background plate (supplied by The Gem Dugout, State College, PA). Diffraction data were collected in the  $3$ – $105^\circ$   $2\theta$  range, sampling with a  $0.02^\circ$  step scan, on a  $\theta:\theta$  vertical scan, using a Bruker AXS D8 Advance diffractometer, equipped with a linear Lynxeye position sensitive detector, set at 300 mm from the sample (Ni-filtered  $\text{Cu K}\alpha_{1,2}$  radiation). Peak search and profile fitting allowed the location of the most prominent, low-angle peaks, which were later used in the indexing process by TOPAS-R (V.3.0, 2005, Bruker AXS, Karlsruhe, Germany); approximate lattice parameters of a primitive orthorhombic cell were determined to be  $a = 38.05 \text{ \AA}$ ,  $b = 7.54 \text{ \AA}$ ,  $c = 9.74 \text{ \AA}$ , and  $\beta = 100.6^\circ$ , with an indexing figure of merit, GOF(20), of 15.1. Systematic absence conditions suggested  $P2_1$  as the probable space group, which was later confirmed by successful structure solution and refinement. Density considerations indicated  $Z = 4$ , thus requiring, for the structure solution process of this crystal phase, the individuation of the center of mass location, orientation, and conformational freedom of two crystallographically independent molecules. In accordance with the material origin and to the crystallization/purification process, this crystal phase contains a number of similar molecules, possessing similar steric requirements. Analytical data, however, suggested that the vast majority of the molecules is represented by  $\beta$ -sitosterol (see the Supporting Information). Therefore, although this crystal phase must be considered as a solid solution of several components, our modeling relies on the use of (two) rigid  $\beta$ -sitosterol fragments (flexible at the alkyl branches), the Cartesian coordinates of which were taken from the crystal structure of a similar species.<sup>33</sup> Real space structure modeling by the simulated annealing algorithm coupled to a Monte Carlo search allowed the definition of a suitable model, later refined by the Rietveld method. All computations were performed by the TOPAS-R suite. The background contribution was modeled by a polynomial fit (Chebyshev model); atomic scattering factors for

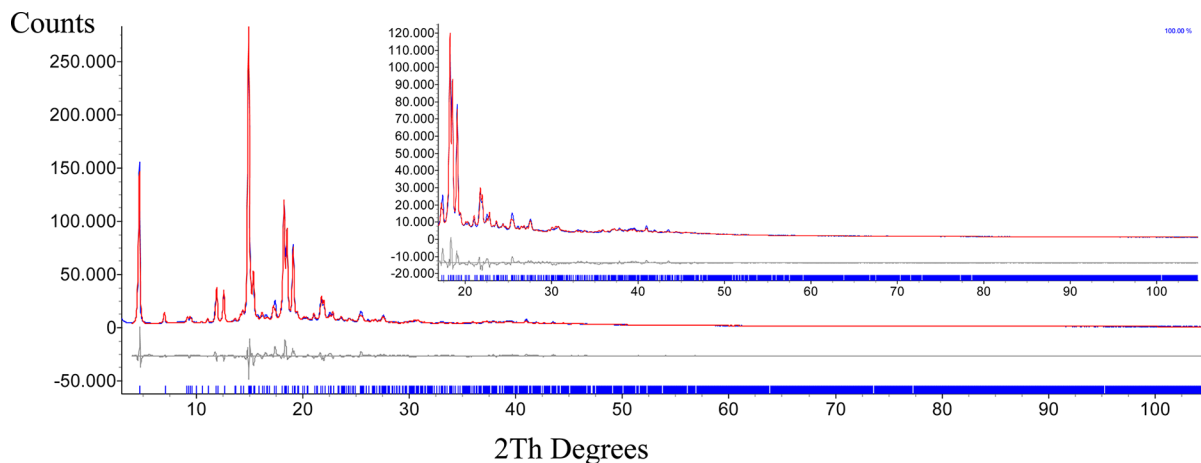


**Figure 4.** Rietveld refinement plot for  $\beta$ -sitosterol, precipitated in the DELOS 5 experiment. Peak markers and difference plot at the bottom. The insert shows the high-angle region at a larger magnification (10 $\times$ ).

**Table 2. Operating Conditions and Outcome in Different DELOS Crystallization Experiments of Phytosterols<sup>a</sup>**

expt	operational conditions					yield (%)	crystallization outcome			UI <sup>e</sup>	crystallinity <sup>f</sup> (%)
	$T_w$ (K)	$C_1^a$ (mol/mol)	$X_{CO_2}^b$	$T_f$ (K)	$\Delta T^c$		$d_{10\%}$	$d_{50\%}$	$d_{90\%}$		
DELOS1	298	$1.7 \times 10^{-3}$	0.36	271	-27	30	1.6	4.7	11.9	13	93
DELOS2	298	$1.7 \times 10^{-3}$	0.46	257	-41	30	1.4	4.1	9.9	14	99
DELOS3	298	$1.7 \times 10^{-3}$	0.56	238	-60	30	2.3	6.5	18.3	12	94
DELOS4	298	$1.7 \times 10^{-3}$	0.64	230	-68	35	1.5	4.1	9.5	16	96
DELOSS	298	$1.7 \times 10^{-3}$	0.77	214	-84	40	0.6	2.3	6.6	9	96
DELOS6	298	$2.3 \times 10^{-3}$	0.46	257	-41	40	1.7	4.8	12.1	14	95
DELOS7	298	$2.3 \times 10^{-3}$	0.55	241	-57	40	1.9	5.7	16.1	12	95
DELOS8	298	$2.3 \times 10^{-3}$	0.64	234	-64	30	1.2	3.5	8.3	14	95
DELOS9	298	$1.1 \times 10^{-3}$	0.46	267	-31	20	1.3	4.0	11.6	11	96
DELOS10	298	$1.7 \times 10^{-3}$	0.46	257	-41	25	1.5	4.6	12.9	11	94
DELOS11	298	$2.3 \times 10^{-3}$	0.46	257	-41	40	1.4	4.4	12.1	11	93
DELOS12	298	$2.9 \times 10^{-3}$	0.45	262	-36	50	1.5	4.9	14.2	10	96
DELOS13	308	$2.3 \times 10^{-3}$	0.76	229	-79	35	1.2	4.1	10.0	12	94
DELOS14	308	$3.8 \times 10^{-3}$	0.45	267	-41	55	1.2	3.8	9.6	12	92

<sup>a</sup> $C_1$  is the concentration of solute in the initial organic solution. <sup>b</sup> $CO_2$  molar fraction in the solvent mixture. <sup>c</sup>Temperature decrease,  $\Delta T = T_f - T_w$ .

<sup>d</sup>Volumetric particle size distribution are described by  $d_{10\%}$ ,  $d_{50\%}$ , and  $d_{90\%}$ , which are the particle diameters ( $\mu\text{m}$ ) under which there are 10%, 50%, and 90% of the total volume of the particles, respectively. <sup>e</sup>Uniformity index is defined as  $UI = d_{10\%}/d_{90\%} \times 100$ . <sup>f</sup>Crystallinity of native-PS in comparison to each DELOS-PS sample calculated as  $\Delta H(\text{native-PS})/\Delta H(\text{DELOS-PS}) \times 100$ .

neutral atoms were taken from the internal library of TOPAS-R. Preferred orientation corrections, in the March–Dollase formulation, were applied on the [100] pole, with final magnitude  $r = 0.929(5)$ . Anisotropic peak broadening, by the spherical harmonics approach, has been tested but lead only to marginally lower agreement factors and was, therefore, abandoned. Figure 4 shows the final Rietveld refinement plot. Fractional atomic coordinates have been deposited as the CIF file within the Cambridge Crystallographic Database as publication no. CCDC 933712.

Crystal data:  $C_{29}H_{50}O$ , fw = 414.71 g mol<sup>-1</sup>, 298 K,  $\lambda$  ( $\text{\AA}$ ) = 1.5418, monoclinic space group  $P2_1$ ,  $a = 37.983(5)$   $\text{\AA}$ ,  $b = 7.5250(6)$   $\text{\AA}$ ,  $c = 9.6957(6)$   $\text{\AA}$ ,  $\beta = 100.49(1)^\circ$ ,  $V = 2724.9(5)$   $\text{\AA}^3$ ,  $Z = 4$ ,  $\rho_{\text{calc}} = 1.011$  g cm<sup>-3</sup>,  $\mu$  (Cu  $K\alpha$ ) = 4.33 cm<sup>-1</sup>,  $R_p = 0.065$ ,  $R_{\text{wp}} = 0.091$ ,  $R_{\text{Bragg}} = 0.037$ .  $2\theta$  range = 4–105°.

### 3. RESULTS AND DISCUSSION

**3.1. Crystallization of Phytosterol Mixture.** The DELOS methodology has arisen in recent years as a powerful technology for the preparation of microparticulate solids with enhanced properties in terms of polymorphic purity and crystal

size homogeneity, not only at the laboratory scale but also at the industrial level.<sup>27–29</sup>

In a previous study, we determined the solubility of phytosterols in  $CO_2$ -expanded ethanol mixtures at different solvent compositions and temperatures.<sup>30</sup> The results demonstrated that the solubility behavior of phytosterols in  $CO_2$ -expanded ethanol exhibits the appropriate characteristics desirable for the DELOS process: phytosterol mixture is soluble in ethanol, and the  $CO_2$  behaves as a cosolvent in a broad range of solvent compositions of up to around the 0.8 mol fraction. Appropriate crystallization conditions of  $X_{CO_2}$  and  $C_1$  were chosen according to the solubility behavior of the phytosterol mixture in  $CO_2$ -expanded ethanol so that in the second step of the DELOS process shown in Figure 2, the  $CO_2$ -expanded mixture would be in the form of a single liquid phase. Such conditions are met below the solubility curve depicted in Figure 3. Consequently, crystallization of the phytosterol mixture was performed from  $CO_2$ -expanded ethanol at 298 K and with a  $X_{CO_2}$  of 0.77 and  $C_1 = 1.7 \times 10^{-3}$  mols phytosterols/mols ethanol (experiment DELOS 5 in Table 2 and Figure 3).

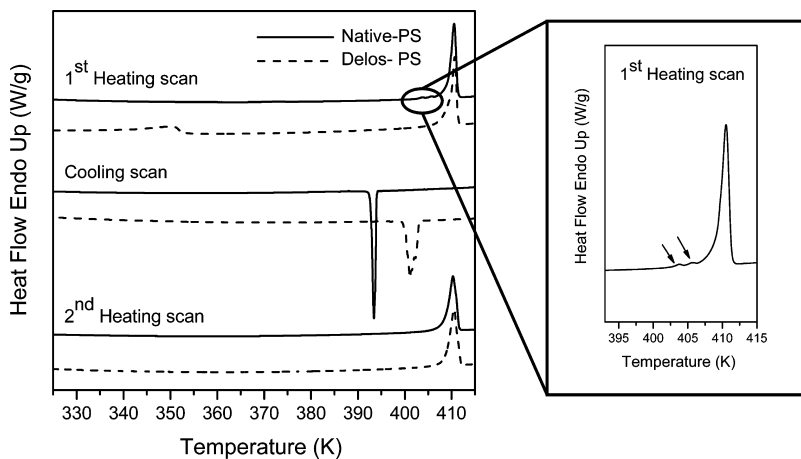


**Figure 5.** DSC traces of native (solid line) and DELOS processed (dotted line) phytosterols. The inset shows the endotherms observed before the melting peak of native phytosterol.

From this experiment, a new and highly crystalline polymorph of phytosterols, which we called DELOS-PS, was obtained in the form of a fine powder with a mean particle diameter of 6.5  $\mu\text{m}$  and narrow particle size distribution. This polymorph was subjected to further detailed characterization.

**3.2. DELOS-PS Polymorph.** **3.2.1. Thermal Behavior.** Representative DSC and TGA curves of the native and the DELOS-PS polymorph are shown in Figures 5 and 6,

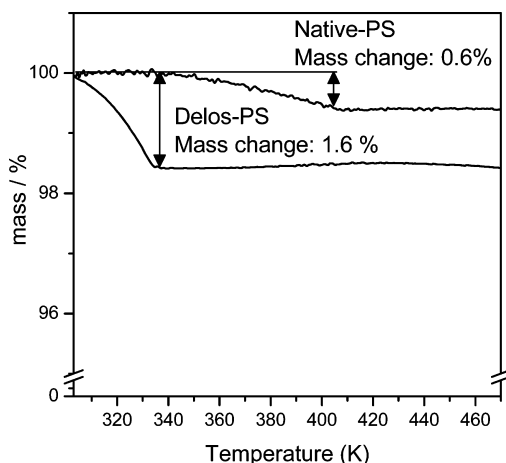


**Figure 6.** TGA traces of native and DELOS processed phytosterols.

respectively. Native phytosterol mixture exhibited two endothermic peaks between 403 and 408 K of very low energy followed by the melting endotherm at  $411.1 \pm 4.7$  K ( $\Delta H = 45 \pm 12$  J/g). The process was also followed by thermo-optical microscopy (TOM, see the Supporting Information). The first two peaks disappeared after cooling and reheating the sample. These peaks could be attributed to the melting of some minor components in the phytosterol mixture (2.9% of the mixture was reported as other unspecified sterols by the manufacturer). A continuous mass loss of 0.6%, probably due to moisture release, was observed by TGA (Figure 6). Similar melting peaks were observed at 411.3 K for  $\beta$ -sitosterol by Christiansen et al.<sup>34</sup> and at 406.3 and 414.5 K for  $\beta$ -sitosterol and sitostanol, respectively, by Melnikov et al.<sup>6</sup>

The DELOS-PS polymorph, however, exhibited two endotherms (Figure 5). The first broad endotherm showed a

maximum peak temperature at  $353.2 \pm 1.8$  K ( $\Delta H = 41 \pm 10$  J/g) that disappeared on the second heating scan. Consistent with the 1.6% mass loss observed in the TGA (Figure 6), this endotherm might correspond to the loss of structural solvent [stoichiometry phytosterol:ethanol (1:0.15)].<sup>35</sup> Similar stoichiometry of sterol–alcohol complexes was reported for cholesterol:ethanol (1:0.42), stigmasterol:ethanol (1:0.18), and stigmasterol:methanol (1:0.50).<sup>36</sup> The second endothermic peak, with an onset temperature at  $409.9 \pm 0.4$  K ( $\Delta H = 47 \pm 2$  J/g), corresponds to melting (as confirmed by TOM, see the Supporting Information), and it is fully reversible on rescan.

A DSC analysis study conducted by Vaikousi et al.<sup>12</sup> on different sterol/stanol mixtures obtained from soy and wood sources also revealed that all samples had narrow melting endotherms between  $411.34 \pm 0.27$  and  $417.72 \pm 0.35$  K ( $\Delta H$  between 39 and 45 J/g), fully reversible on rescan, regardless of the plant origin. A smaller and broader endothermic transition at 370–378 K range that indicated the presence of a different crystal type was also observed. Similar melting peaks at 373 and 413 K were observed by Kalkura and Devanarayanan<sup>37</sup> during DSC analysis of  $\beta$ -sitosterol crystals grown on silica gel and attributed to the loss of hydration water and melting of crystals, respectively. Thermograms for  $\beta$ -sitosterol precipitated from the acetone–water mixture revealed two wide endothermic peaks at temperatures below the original melting peak. The transitions corresponded to the dehydration of  $\beta$ -sitosterol monohydrate occurring in two separate stages; first half of the hydration water is eliminated and a hemihydrate crystal is formed (below 333 K), while at the second dehydration stage the rest of the hydration water is lost below 363 K. Following a CO<sub>2</sub>-based process, Turk et al.<sup>24</sup> showed the micronized phytosterol powder obtained from the RESS process to have a lower melting temperature (peak in the range of 403 to 415 K) and heat of fusion (~46 J/g) compared to the unprocessed sample.

Note that in the DELOS-PS polymorph the endotherms associated with the melting of the minor components observed in the native form between 403 and 408 K did not appear. This could be attributed to a subtle purification of the phytosterol mixture after DELOS crystallization, as suggested by HPLC analysis (see the Supporting Information). Within the temperature range from 298 to 473 K, this compound either in native or recrystallized form does not decompose.

**3.2.2. Comparative Crystal Chemistry.** Several reports deal with the crystalline phases of  $\beta$ -sitosterol.<sup>10,34,35,38</sup> To date, anhydrous, hemihydrate, and monohydrate forms have been prepared. The monohydrate form can be prepared by cooling hot saturated solutions of acetone/water (95:5, v/v). The hemihydrate form can be produced by either drying the monohydrate or by crystallization under regulation of water concentration at the parts per million level in the water-immiscible solvent hexane.<sup>35</sup> The anhydrous form can be directly crystallized from dry acetone solutions or it can be obtained by complete dehydration of the monohydrate phase at room temperature. However, even though different polymorphs have been identified, the only crystal structure determined so far is that of  $\beta$ -sitosterol monohydrate.<sup>38</sup> Simulation of the XRPD patterns available from the published atomic coordinates of  $\beta$ -sitosterol monohydrate did not reveal any match to that of native-PS or the DELOS-PS (see the Supporting Information) polymorphs described in this study. A variety of XRPD traces of  $\beta$ -sitosterol, sitostanol, and plant sterols from wood pulp and vegetable oils was also reported,<sup>6</sup> but none matched the experimental traces obtained in this study. Other recent observations confirmed the versatility of this system: Vaikousi et al.<sup>12</sup> showed marked differences in the XRPD traces of sterol versus stanol mixtures, even though patterns of samples originating from soy or wood in each category were found to be similar. Rossi et al.<sup>11</sup> observed a change in the diffraction pattern between the starting phytosterol mixture and the colloidal particles obtained after antisolvent precipitation with water, a lower degree of crystallinity being observed in the latter case. Also, Turk et al.<sup>24</sup> reported a decrease in the crystallinity of phytosterols upon micronization with the RESS methodology.

In contrast, the XRPD patterns recorded in this study and displayed in Figure 7 demonstrated that crystallization by

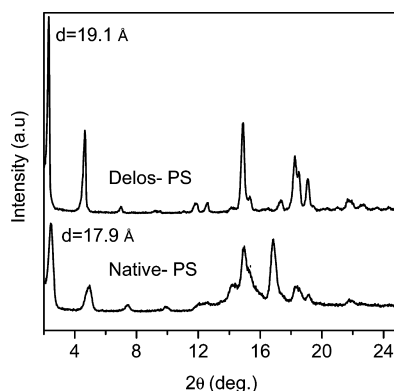


**Figure 7.** X-ray powder diffraction patterns of native-PS and DELOS-PS solids at angular range 2–25 ( $2\theta$ ).

DELOS transforms native-PS into a distinct polymorph of much higher crystallinity. These newly isolated DELOS-PS samples manifest a significant shift of the low-angle reflections to lower  $2\theta$  values, indicating that the longest axis, compared to that of the native sterol polymorph, is expanded (for the actual refined value, see Section 2.3.5 above). Significantly, the reduced background intensity and the narrower peak breadth in the DELOS-PS phase, indicated, beyond the likely lowering of amorphous material, a relatively higher crystallinity, possibly reducing the rate of solubilization. Indeed, the degree of crystallinity reported in Table 2 of native-PS with respect to

each DELOS-PS samples is slightly lower than 100%, regardless of the process conditions.

**3.2.3. Polymorphic Transitions and Crystal Packing.** As anticipated, the polymorphism of sterol compounds is rather complex due to the similarity of the sterol/stanol molecular structures and to the difficulties in isolating crystal phases of analytically pure molecular species. The two polymorphs characterized in this study are chemically and structurally related. Indeed, spontaneous elimination of residual ethanol from the DELOS-PS polymorph after a 2-year storage period at room temperature retains the original crystal form (Figure 8a).

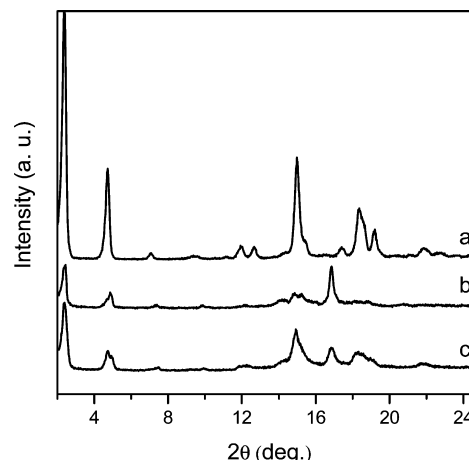


**Figure 8.** X-ray powder diffraction patterns of DELOS-PS polymorph recorded after (a) storing the sample at room temperature for 2 years, (b) melting in a Pyrex tube followed by spontaneous recrystallization at room temperature, and (c) aging at 368 K for 7 h.

Instead, the fast elimination of the ca. 1.6% of residual ethanol from the DELOS-PS polymorph, either by melting and recrystallization at room temperature (Figure 8b) or by aging at 368 K for 7 h (Figure 8c), leads to transformation into the native-PS polymorph. Consequently, transformation between both polymorphs should be kinetically driven.

The crystal structure of the DELOS-PS polymorph, here for simplicity attributed to  $\beta$ -sitosterol (by far the major component, as evidenced by HPLC analysis data, see the Supporting Information), was determined from high-quality XRPD data. The DELOS-PS polymorph is monoclinic,  $P2_1$ , and contains two crystallographic independent steroid molecules. This was not unexpected, since similar structures, sharing the same space group and manifesting comparable lattice metrics, are known in the literature.<sup>39,40</sup> In addition, a number of closely related species,<sup>41</sup> although crystallizing in different space groups, show cell parameters reminiscent of the case under study, some with doubling of the long(est) (ca. 38 Å) cell axis in I-centered monoclinic lattices. As it is well-known, powder diffraction data, particularly on less-than-ideal materials, do not allow the use of the independent atom model during structure solution nor in the final refinements. This is particularly true for moderately complex organic materials, where the rapid falloff of the scattering power, relatively high thermal parameters and unavoidable (and extreme) peak overlap (beyond, say, 30°  $2\theta$ ) require the introduction of many (mostly geometrical) restraints (from external observations), or, even better, rigid bodies (flexible at a few saturated, acyclic bonds). The latter choice, adopted in this study, allowed

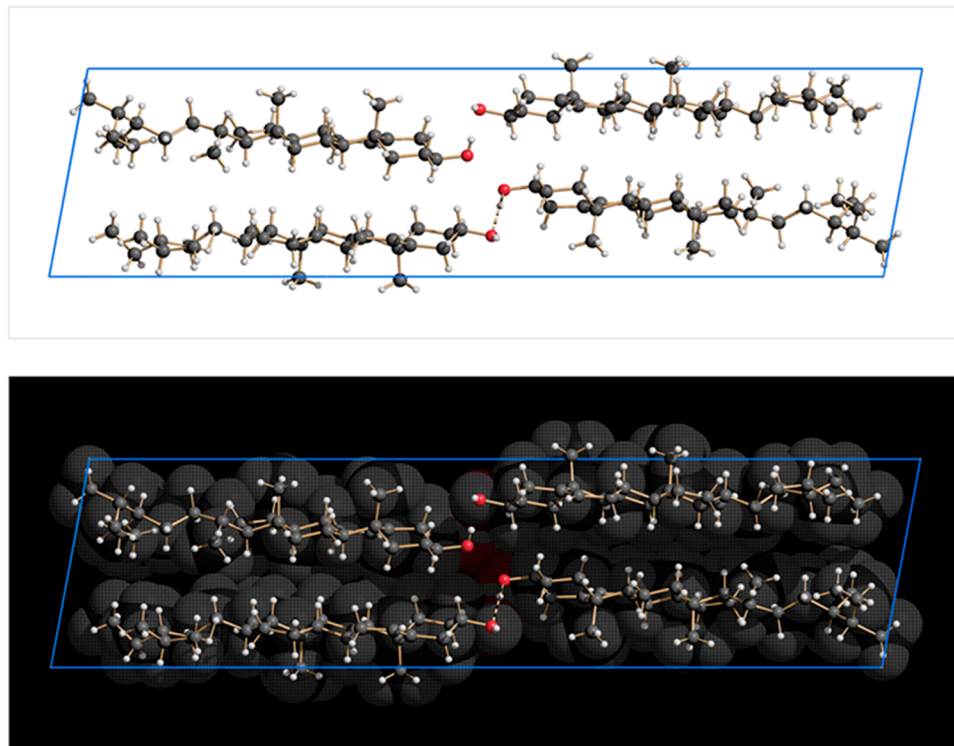


**Figure 9.** Crystal packing diagram for the structure of  $\beta$ -sitosterol, viewed down [010]. Horizontal axis is (a). Top: wireframe representation, highlighting the intermolecular OH...O interaction (fragmented line). Bottom: space-filling model showing the mutual interlocking of the two crystallographically independent molecules (in  $P2_1$ ,  $Z = 4$ ) in the unit cell.

the definition of a reasonably accurate model (Figure 9), where an intermolecular OH...O bond ( $2.90 \text{ \AA}$ ) can be observed.

Interestingly, analytical data suggest the presence, in the crystalline material, of some vicariant molecules, some of them with slightly smaller alkyl branches. While this effect may be responsible for the partial broadening of the diffraction peaks (due to local strain fields), a few cavities in the crystal structure may be occasionally formed. This is somewhat in agreement with the observation of some residual solvent molecules (specifically, ethanol), which, trapped near the crystal defects in the ideal  $\beta$ -sitosterol lattice, cannot be detected by diffraction methods but are easily seen by other experimental techniques (TG analyses, above all). It is experimentally observed that with sufficiently long storage times of up to 2 years, vicariant solvent molecules are spontaneously eliminated without modifying the crystal packing.

**3.2.4. Particle Morphology.** The size and crystal morphology largely affect crystal aggregation phenomena and rheological properties, thereby influencing the sensorial attributes of each phytosterol polymorph as well as physiological efficacy. Several morphologies are described for phytosterols. Rossi et al.<sup>11</sup> obtained rod-shaped colloidal particles by antisolvent precipitation in water. Particles had an average aspect ratio ( $L/D$  ratio) of 3–4 within a range of 3–20 caused by high polydispersion ( $L = 500\text{--}700 \text{ nm}$ ,  $D = 80\text{--}250 \text{ nm}$ ). Rodlike crystals were also reported by Christiansen et al.<sup>10</sup> when  $\beta$ -sitosterol was crystallized from an oil solution. On the other hand, Kawachi et al.<sup>35</sup> observed both rodlike and platelike morphologies for crystals obtained from a hexane solution. Turk et al.<sup>24</sup> also presented a SEM micrograph of the unprocessed phytosterol mixture (83%  $\beta$ -sitosterol), which looks somewhat similar to those in this study, with a mix of plates and rods. After the RESS process, agglomerates of fine

particles with particle size of around 50 nm were formed using pre-expansion temperature of 388 K and a pressure of 20 MPa. Such a high temperature was used by Turk et al.<sup>24</sup> to achieve a single phase of the  $\text{CO}_2$ /phytosterol/L-PLA mixture prior to expansion in order to form composite particles using RESS.

The morphology of the DELOS-PS and native-PS particles evaluated by scanning electron microscopy is shown in Figure 10. In the original sample, rod- and platelike small size crystals of sterols of up to  $50 \mu\text{m}$  aggregate into globular clusters of

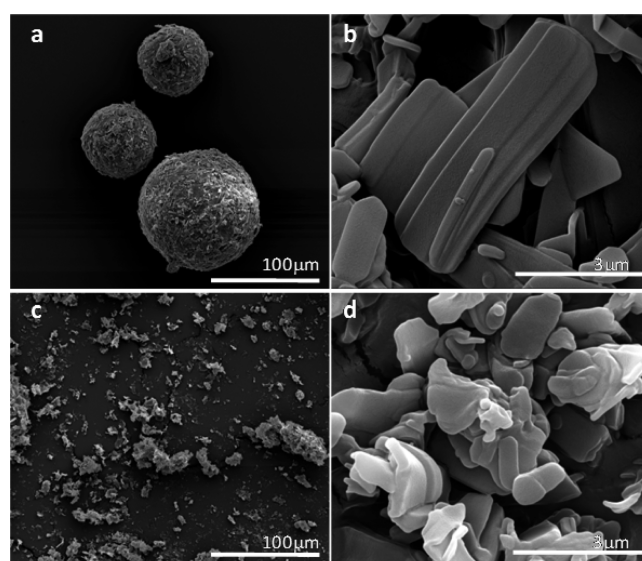


**Figure 10.** Scanning electron micrographs of phytosterol crystals before (images a and b) and after (images c and d) recrystallization with the DELOS process.

around 100  $\mu\text{m}$  diameter. Even though the details of the industrial manufacturing process are not known, it is possible that spray drying may have been used in the final step to generate such a globular shape of the native phytosterol sample. In contrast, the DELOS-PS particles show micrometric platelike crystals with rounded edges, thickness between 150 and 450 nm, and a low aspect ratio. These elongated crystals aggregate as shapeless clusters.

### 3.3. Effect of Process Parameters on Crystallization Outcome.

The influence of the operational parameters  $X_{\text{CO}_2}$  and  $C_1$  on the crystallization yield and particle size was also investigated. Distinct sets of experiments at 298 and 308 K using different  $C_1$  and  $X_{\text{CO}_2}$  levels were performed. Three sets of experiments were designed at  $P_w$  of 10 MPa and  $T_w$  of 298 K: (a) keeping initial concentration ( $C_1$ ) constant at  $1.7 \times 10^{-3}$ , below the saturation limit of phytosterol mixture in ethanol, and varying  $X_{\text{CO}_2}$  over the range of 0.35–0.80, (b) keeping initial concentration ( $C_1$ ) constant at  $2.3 \times 10^{-3}$ , above the saturation limit of the phytosterol mixture in ethanol, and varying  $X_{\text{CO}_2}$  from 0.45 to 0.65, and (c) keeping  $X_{\text{CO}_2}$  constant at 0.45 and varying the  $C_1$  over the range from 0.6 to 1.5. As illustrated in Figure 3, in all these experiments, the operational parameters were carefully selected in order to ensure that the phytosterol mixture in  $\text{CO}_2$ -expanded ethanol (second step of the DELOS process, Figure 2) would be in the form of a single liquid phase. Such conditions are met below the solubility curve of phytosterol mixture, in  $\text{CO}_2$ -expanded ethanol, depicted in Figure 3.

Table 2 provides information on the operating conditions and the outcome of each crystallization experiment in terms of yield, particle size distribution, and crystallinity. In all experiments, micrometer-sized crystalline powders were produced with a XRP diffractogram corresponding to the DELOS-PS phase. This result confirmed, once again, the high robustness of supercritical fluid technology for producing highly pure crystalline forms of compounds showing complex polymorphism.<sup>27,42,43</sup>

The results, summarized in Table 2, indicated that the crystallization yield is highly dependent on the initial concentration,  $C_1$ , but it does not vary significantly by changing the  $\text{CO}_2$  content in the mixture. This peculiar behavior can be explained taking into account the solubility variation of phytosterols with temperature. Indeed, under the conditions of the DELOS crystallization (Figure 2), extensively described in reference 29, it could be considered that the difference between the initial concentration,  $C_1$ , of the solution and the solute solubility in the conventional solvent at the final temperature,  $T_f$ , achieved upon depressurization,  $C_F^S$ , is the maximum supersaturation that can be achieved,  $\Delta C$  ( $\Delta C = C_1 - C_F^S$ ). Consequently, the higher the  $\Delta C$ , the higher the maximum supersaturation reached, and the higher crystallization yield attained. This concept was used before to rationalize the crystallization outcome of cholesterol from  $\text{CO}_2$ -expanded acetone following the same crystallization procedure.<sup>29</sup>

The solubility in ethanol of  $\beta$ -sitosterol, main component of the native phytosterol mixture, increases exponentially with temperature. But there is no significant change in solubility at temperatures below 278 K.<sup>44</sup> The increase in the  $\text{CO}_2$  content in experiments DELOS1 to DELOSS results in a decrease in the final temperature ( $T_f$ ), from 271 K in DELOS1 to 214 K in DELOSS. However, in this case such a temperature drop will not affect the maximum supersaturation achieved,  $\Delta C$ , since the solubility of PS in ethanol at temperatures below 278 K,  $C_F^S$ , is

expected to remain approximately constant and all these experiments were performed at the same  $C_1$ . This resulted in similar crystallization yields regardless of the  $\text{CO}_2$  content. The same behavior is observed in experiments DELOS6–8. However, the situation changes in experiments DELOS9–12, in which the  $\text{CO}_2$  molar fraction is kept constant while the initial concentration,  $C_1$ , is increased. Under these conditions, the depressurization step provokes in all cases a similar temperature drop between 30 and 40 K. Despite  $T_f$  and  $C_F^S$  remain nearly constant, in all four experiments, the increase of the initial concentration  $C_1$  causes the production of a much more powerful supersaturation increase,  $\Delta C$ , during the depressurization step and the attainment of higher crystallization yields.

Experiments were also performed at 308 K (DELOS13 and DELOS14) at the two extreme points of  $X_{\text{CO}_2}$  and  $C_1$ . As expected, the yield was higher at  $C_1$  of  $3.8 \times 10^{-3}$  mol/mol and also higher than that at 298 K, probably due to the increased solubility of phytosterols in the ethanol +  $\text{CO}_2$  mixture<sup>30</sup> produced by the synergistic effect between ethanol and  $\text{CO}_2$ .

Particle size distribution of solids obtained under the studied conditions is also presented in Table 2. The mean particle diameter ( $d_{50\%}$ ) for the starting material was 188  $\mu\text{m}$  with a wide particle size distribution (uniformity index, UI = 0.6). The appearance of the particles was globular and free-flowing, reflecting the treatments applied during the proprietary manufacturing process. The particles yielded by the DELOS process were substantially smaller in size with  $d_{50\%}$  being between 2.3 and 6.5  $\mu\text{m}$  for all the conditions investigated. Even though there was no clear trend, the smallest particles were produced at  $X_{\text{CO}_2}$  of 0.77 and  $C_1$  of  $1.7 \times 10^{-3}$  mol/mol, corresponding to the largest temperature drop of –84 degrees (experiment DELOSS). Such a large, uniform, and instantaneous temperature drop leads to the formation of small particles with a narrow particle size distribution. The uniformity of the particle size distribution obtained under the majority of the conditions was in the range of 9–16, reflecting the high level of homogeneity achieved. Smaller particles were produced by Turk and Leitzow<sup>25</sup> using the RESSAS process. Using Tween80, their particles showed an average size of 270 nm but decreased to 50 nm when the surfactant used was SDS (sodium dodecyl sulfate) possibly due to the lower dynamic interfacial tension of SDS. No such surfactants were used during the DELOS process employed in this study.

In order to check process reproducibility, experiment DELOS4 has been repeated three times. In all batches, pure DELOS-PS polymorph was produced and excellent reproducibility was also achieved in terms of temperature decrease ( $-68 \pm 3$  K), crystallization yield ( $35 \pm 5\%$ ), and particle size ( $d_{50\%} = 4 \pm 0.8 \mu\text{m}$ ; UI =  $16 \pm 4$ ).

One of the challenges in large-scale crystallization procedures is batch-to-batch reproducibility. Compared with conventional crystallizations from liquid solvents, the inherent features of crystallization from  $\text{CO}_2$ -expanded solvents make it very easy to scale up, avoiding common scaling-up troubles such as those related to agitation.<sup>29</sup> In conventional batch cooling crystallizations, the stirring rate and the stirrer design determine the supersaturation homogeneity and therefore the homogeneity in particle characteristics (polymorphism, size, and morphology). When scaling up, this parameter becomes critical: the bigger the crystallization vessel, the bigger the temperature gradient from the vessel walls to the center, giving very heterogeneous supersaturation profiles and poor reproducibility, which

complicates potential scale-up. Since in the DELOS process stirring is only used in the pressurization step, to achieve a faster mixing of the CO<sub>2</sub> with the organic solvent, and it is not needed in the depressurization step, where the crystallization occurs, the homogeneity of the supersaturation achieved is independent of the vessel volume and the stirring rate does not affect the final characteristics of the crystalline particles.

#### 4. CONCLUSIONS

The findings of this study demonstrate the production of a new micrometer-sized polymorph of phytosterol using a simple and scalable method, which employs a bottom-up approach based on the use of CO<sub>2</sub>-expanded ethanol as the solvent media. Particle size of the phytosterol crystals was reduced from 188 μm to <6.5 μm with a narrow size distribution at all processing conditions employed. The new phase shows higher chemical purity and higher crystallinity than the native mixture. It is stable at room temperature at least for 2 years but can be converted into the native form by heating it above 368 K. The crystal structure of the new polymorph is reported for the first time. In cases like this one, when single crystals of suitable size and quality are not available, the only viable method toward structure solution is XRPD analysis, which, for molecular compounds of moderate complexity, has been shown to afford relevant structural information, otherwise inaccessible. While the accuracy of this method is significantly lower than conventional diffraction methods, nevertheless, important features, like packing preferences, are well-determined.

Further studies are now needed to confirm the expected enhancement of adsorption and bioavailability of phytosterols due to size reduction as well as to compare the efficacy of the new phytosterol polymorph.

#### ■ ASSOCIATED CONTENT

##### Supporting Information

Thermo-optical characterization of native and DELOS-PS polymorphs, powder X-ray diffraction of the crystal structure of β-sitosterol monohydrate in comparison to native, and DELOS-PS phases and characterization of the composition of native-PS and DELOS-PS samples by HPLC analyses are available free of charge via the Internet at <http://pubs.acs.org>.

#### ■ AUTHOR INFORMATION

##### Corresponding Authors

\*E-mail: feral.temelli@ualberta.ca. Tel: 1-780-492-3829. Fax 1-780-492-8914.

\*E-mail: ventosa@icmab.es. Tel: 34-93-580-1853. Fax: 34-93-580-5729.

##### Notes

The authors declare no competing financial interest.

#### ■ ACKNOWLEDGMENTS

F.T. is grateful for the Grant for Foreign Researchers and Professors from AGAUR of the Catalan Government. E.M.-C. acknowledges the MICINN for a Juan de la Cierva postdoctoral contract. Thank you to Arboris Pine Tree Extracts for providing the phytosterol sample. This work was supported by grants from DGI, Spain, project POMAS (Grant CTQ2010-019501) and DGR, Catalunya (project 2005SGR 00591). The authors appreciate the financial support through the project "Development of nanomedicines for enzymatic replacement therapy in Fabry disease" granted by the Fundació Marató TV3. We also

acknowledge financial support from Instituto de Salud Carlos III, through "Acciones CIBER". The Networking Research Center on Bioengineering, Biomaterials and Nanomedicine (CIBER-BBN) is an initiative funded by the VI National R&D&I Plan 2008–2011, Iniciativa Ingenio 2010, Consolider Program, CIBER Actions and financed by the Instituto de Salud Carlos III with assistance from the European Regional Development Fund.

#### ■ REFERENCES

- (1) Katan, M. b.; Grundy, S. M.; Jones, P.; Law, M.; Miettinen, T.; Paoletti, R. *Mayo Clin. Proc.* **2003**, *78*, 965.
- (2) Health claims: Plant sterol/stanol esters and risk of coronary heart disease (CHD); 21CFR101.83; FDA: Silver Spring, MD, 2010.
- (3) Scientific Opinion of the Panel on Dietetic Products Nutrition and Allergies on a request from Unilever PLC/NV on Plant Sterols and lower/reduced blood cholesterol, reduced the risk of (coronary) heart disease. *EFSA J.* **2008**, *781*, 1.
- (4) Jahreis, G.; Wohlgemuth, S.; Grünz, G.; Martin, L.; Knieling, M.; Engel, R.; Türk, M.; Keller, S. *Nanomedicine: Nanotechnology, Biology and Medicine* **2013**, DOI: 10.1016/j.nano.2013.03.007.
- (5) Melnikov, S. M.; Seijen ten Hoorn, J. W. M.; Eijkelenboom, A. P. *A. M. Chem. Phys. Lipids* **2004**, *127*, 121.
- (6) Melnikov, S. M.; Seijen ten Hoorn, J. W.; Bertrand, B. *Chem. Phys. Lipids* **2004**, *127*, 15.
- (7) Rozner, S.; Garti, N. *Colloids Surf., A* **2006**, *435*, 282–283.
- (8) Ostlund, R. E. *Annu. Rev. Nutr.* **2002**, *22*, 533.
- (9) Piironen, V.; Lindsay, D. G.; Miettinen, T. A.; Toivo, J.; Lampi, A. M. *J. Sci. Food Agric.* **2000**, *80*, 939.
- (10) Christiansen, L. I.; Rantanen, J. T.; Von Bonsdorff, A. K.; Karjalainen, M. A.; Yliruusi, J. K. *Eur. J. Pharm. Sci.* **2002**, *15*, 261.
- (11) Rossi, L.; Ten Hoorn, J. W. M.; Melnikov, S. S. M.; Velikov, K. P. *Soft Matter* **2010**, *6*, 928.
- (12) Vaikousi, H.; Lazaridou, A.; Biliaderis, C. G.; Zawistowski, J. J. *Agric. Food Chem.* **2007**, *55*, 1790.
- (13) Salo, P.; Wester, I. *Am. J. Cardiol.* **2005**, *96*, 51.
- (14) Leong, W. F.; Man, Y. B. C.; Lai, O. M.; Long, K.; Misran, M.; Tan, C. P. *J. Agric. Food Chem.* **2009**, *57*, 8426.
- (15) Engel, R.; Knorr, D. *Eng. Life Sci.* **2004**, *4*, 374.
- (16) Engel, R.; Schubert, H. *Innov. Food Sci. Emerging Technol.* **2005**, *6*, 233.
- (17) Ostlund, R. E. J.; Spilburg, C. A.; Stenson, W. F. *Am. J. Clin. Nutr.* **1999**, *70*, 826.
- (18) Rozner, S.; Verkhovski, L.; Nissimov, Y.; Aserin, A.; Vilensky, R.; Danino, D.; Zouboulis, C.; Milner, Y.; Garti, N. *Chem. Phys. Lipids* **2008**, *153*, 109.
- (19) Vázquez, L.; Torres, C. F.; Fornari, T.; Grigelmo, N.; Señoráns, F. J.; Reglero, G. *Eur. J. Lipid Sci. Technol.* **2006**, *108*, 659.
- (20) Torres, C. F.; Fornari, T.; Torrela, G.; Senorans, F. J.; Reglero, G. *Eur. J. Lipid Sci. Tech.* **2009**, *111*, 459.
- (21) Guclu-Ustundag, O.; Temelli, F. *J. Am. Oil Chem. Soc.* **2007**, *84*, 953.
- (22) Dunford, N. T.; Teel, J. A.; King, J. W. *Food Res. Int.* **2003**, *36*, 175.
- (23) Jung, J.; Perrut, M. *J. Supercrit. Fluids* **2001**, *20*, 179.
- (24) Turk, M.; Upper, G.; Hils, P. *J. Supercrit. Fluids* **2006**, *39*, 253.
- (25) Turk, M.; Lietzow, R. *J. Supercrit. Fluids* **2008**, *45*, 346.
- (26) Ventosa, N.; Sala, S.; Veciana, J. *J. Supercrit. Fluids* **2003**, *26*, 33.
- (27) Sala, S.; Elizondo, E.; Moreno, E.; Calvet, T.; Cuevas-Diarte, M. A.; Ventosa, N.; Veciana, J. *Cryst. Growth Des.* **2010**, *10*, 1226.
- (28) Gimeno, M.; Ventosa, N.; Sala, S.; Veciana, J. *Cryst. Growth Des.* **2006**, *6*, 23.
- (29) Sala, S.; Córdoba, A.; Moreno-Calvo, E.; Elizondo, E.; Muntó, M.; Rojas, P. E.; Larrayoz, M. Á.; Ventosa, N.; Veciana, J. *Cryst. Growth Des.* **2012**, *12*, 1717.
- (30) Temelli, F.; Córdoba, A.; Elizondo, E.; Cano-Sarabia, M.; Veciana, J.; Ventosa, N. *J. Supercrit. Fluids* **2012**, *63*, 59.
- (31) Ventosa, N.; Sala, S.; Veciana, J. *Cryst. Growth Des.* **2001**, *1*, 299.

- (32) Lemmon, E. W.; McLinden, M. O.; Friend, D. G. Thermophysical Properties of Fluid Systems. In *NIST Chemistry WebBook, NIST Standard Reference Database Number 69*; Linstrom, P.J., Mallard, W.G., Eds.; National Institute of Standards and Technology: Gaithersburg, MD, 2010 (<http://webbook.nist.gov>).
- (33) Petit, G. R.; Numata, A.; Cragg, G. M.; Herald, D. L.; Takada, T.; Iwamoto, C.; Riesen, R.; Schmidt, J. M.; Doubek, M. L.; Goswami, A. *J. Nat. Prod.* **2000**, *63*, 72.
- (34) Christiansen, L.; Karjalainen, M.; Seppänen-Laakso, T.; Hiltunen, R.; Yliruusi, J. *Int. J. Pharm.* **2003**, *254*, 155.
- (35) Kawachi, H.; Tanaka, R.; Hirano, M.; Igarashi, K.; Ooshima, H. *J. Chem. Eng. Jpn.* **2006**, *39*, 869.
- (36) Wong, J. M.; Johnston, K. P. *Biotechnol. Prog.* **1986**, *2*, 29.
- (37) Kalkura, S. N.; Devanarayanan, S. *J. Mater. Sci. Lett.* **1989**, *8*, 481.
- (38) Argay, G.; Kálmán, A.; Vladimirov, S.; Zivanov-Stakic, D.; Ribár, B.  $C_{29}H_{52}O_2$ . *Z. Kristallogr.* **1996**, *211*, 725.
- (39) Wendorff, J. H.; Price, F. P. *Mol. Cryst. Liq. Cryst.* **1974**, *25*, 71.
- (40) Subash-Babu, P.; Ignacimuthu, S.; Agastian, P.; Varghese, B. *Bioorg. Med. Chem.* **2009**, *17*, 2864.
- (41) Bernal, J. D.; Crowfoot, D.; Fankuchen, I. *Philos. Trans. R. Soc., A* **1940**, *239*, 135.
- (42) Brun, G. W.; Martin, A.; Cassel, E.; Vargas, R. M. F.; Cocero, M. *J. Cryst. Growth Des.* **2012**, *12* (4), 1943.
- (43) Bouchard, A.; Jovanovic, N.; Hofland, G. W.; Mendes, E.; Crommelin, D. A. J.; Jiskoot, W.; Witkamp, G.-J. *J. Cryst. Growth Des.* **2007**, *7* (8), 1432.
- (44) Wei, D.; Wang, L.; Liu, C.; Wang, B. *J. Chem. Eng. Data* **2010**, *55*, 2917.
- (45) Armstrong, M. J.; Carey, M. C. *J. Lipid Res.* **1987**, *28*, 1144.